

Breast Cancer Classification Based on Mammogram Images Using CNN Method with NASNet Mobile Model

Diah Devi Pramesti¹, Yuniar Farida^{*2}, Dian Candra Rini Novitasari³, Achmad Teguh Wibowo⁴

^{1,2,3,4}Universitas Islam Negeri Sunan Ampel, Surabaya, Indonesia

e-mail: ¹diahdevi92@gmail.com, ^{*2}yuniar_farida@uinsa.ac.id, ³diancrini@uinsa.ac.id,

⁴atw@uinsa.ac.id

Abstrak

Di Indonesia, jenis kanker yang menyumbang tingkat kematian tertinggi adalah kanker payudara, sehingga membutuhkan pemeriksaan dini, pemeriksaan klinis, dan skrining, termasuk mamografi. Mamografi saat ini adalah metode paling efektif untuk mendeteksi kanker payudara pada tahap awal. Penelitian ini bertujuan untuk mengklasifikasikan sel kanker payudara berdasarkan gambar mamogram. Metode yang digunakan dalam penelitian ini adalah CNN (Convolutional Neural Network) dengan model NASNet Mobile untuk mengklasifikasikan tiga kelas: normal, jinak, dan ganas. Metode CNN dapat mempelajari berbagai atribut input secara kuat sehingga CNN dapat memperoleh karakteristik data yang lebih detail dan memiliki kemampuan deteksi yang lebih baik. Penelitian ini memperoleh model paling optimal berdasarkan persentase nilai akurasi, sensitivitas, dan spesifitas masing-masing sebesar 99,67%, 98,78%, dan 99,35%. Penelitian ini dapat digunakan untuk membantu radiolog sebagai pertimbangan dalam mengambil keputusan diagnosis kanker payudara.

Kata kunci— Kanker Payudara, CNN, Deep Learning, NASNet Mobile, Gambar Mamografi

Abstract

In Indonesia, the type of cancer that contributes to the highest death rate is breast cancer, so it requires early examination, clinical examination, and screening, which includes mammography. Mammography is currently the most effective method for detecting early-stage breast cancer. This study aims to classify breast cancer cells based on mammogram images. The technique used in this research is CNN (Convolutional Neural Network) with the NASNet Mobile model for classifying three classes: normal, benign, and malignant. The CNN method can learn various input attributes powerfully so that CNN can obtain more detailed data characteristics and has better detection capabilities. This research received the most optimal model based on the percentage of accuracy, sensitivity, and specificity values of 99.67%, 98.78%, and 99.35%, respectively. This research can be used to help radiologists as considerations in making breast cancer diagnosis decisions.

Keywords— Breast Cancer, CNN, Deep Learning, NASNet Mobile, Mammogram Image

1. INTRODUCTION

Cancer is one of the leading causes of death globally, claiming nearly 10 million lives in 2020, according to WHO. Breast cancer is among the most common types, with 68,858 new cases reported in Indonesia and over 22,000 deaths, 70% of which were detected at an advanced stage [1,2]. Early detection through screening methods such as mammography is crucial to

reduce mortality [3]. As the most effective early screening tool, mammography provides detailed X-ray images that help identify benign and malignant tumors. Benign tumors are noncancerous, grow slowly, do not spread to surrounding tissues, and are generally not life-threatening. In contrast, malignant tumors are cancers characterized by rapid and invasive growth of abnormal cells and the ability to spread (metastasize) to other organs via the bloodstream or lymphatic system. Early and accurate diagnosis to distinguish between these two types of tumors is crucial in determining treatment strategies, ranging from routine observation to aggressive oncological intervention [4]. This study focuses on classifying mammogram images into three classes: normal, benign, and malignant tumors, without involving tumor localization or segmentation processes.

Abnormalities are commonly detected through masses or microcalcifications visible in mammogram images. Microcalcifications can indicate breast cancer [5], though interpretation is often challenging due to variability in tissue structure, shape, orientation, size, and brightness. These variations can make it difficult for medical professionals to interpret mammograms accurately [6]. With advances in technology, diagnostic processes are increasingly supported by Artificial Intelligence (AI), particularly through deep learning methods proven effective for various classification tasks, including image, video, and text classification [9,10].

Some methods in deep learning include Artificial Neural Network (ANN), Recurrent Neural Network (RNN), and Convolutional Neural Network (CNN) [11,12]. CNNs are exceptionally robust in learning spatial features, outperforming ANN and DNN. Zhang et al. [11] reported CNN achieving a 99.8% AUC for ultrasonic signal classification, surpassing RNN (96.1%) and DNN (98.7%).

Popular CNN architectures include VGG-16, VGG-19, MobileNet-V1, Xception, AlexNet, GoogleNet, Inception V3, ResNet, and NASNet [19]. NASNet has shown excellent accuracy and faster computation times than many of these models. Furthermore, NASNet also exhibits a speedier computation time than other CNN methods [13]. In addition to having fast computation time, NASNet demonstrates efficiency and a simpler algorithm than several other CNN architectures, such as ResNet, Xception, Inception-ResNet-v2, Inception-v2, and Inception-v3. Sadad et al. [14] reported that NASNet Mobile achieved 99.6% accuracy in brain tumor detection, outperforming MobileNet (91.8%), Inception (92.8%), ResNet (92.9%), and DenseNet (93.1%). K. Radhika [15] demonstrated NASNet's superiority over VGG19, ResNet50, and MobileNet in ear recognition tasks.

NASNet is divided into two architectural models, NASNet Large and NASNet Mobile [16]. The NASNet Large and NASNet Mobile architectures have respective input image sizes of 331×331 and 224×224 . NASNet Mobile uses fewer parameters, specifically 5.3 million, than NASNet Large, which has 8.9 million. Consequently, the required computation time for NASNet Mobile is faster than that of NASNet Large [17]. Nevertheless, NASNet Mobile is capable of achieving better accuracy than NASNet Large. Subrato Bharati [16] compared NASNet Mobile and NASNet Large for COVID-19 diagnosis, with NASNet Mobile yielding superior results. The accuracy achieved using NASNet Mobile was 82.4%, while NASNet Large only reached 81.1%.

Based on the Advantages of the CNN NASNet model in previous studies, this study employs the CNN model NASNet Mobile to classify breast cancer based on mammogram images. The research contributes to facilitating medical professionals in the diagnosis of breast cancer.

2. METHODS

There are five main stages in image classification for breast cancer: data collection, pre-processing, model design, training, and classification. For the design stage, the CNN model evaluated in this study is NASNet Mobile [10]. Using K-Fold cross-validation, samples are

divided into two sets, namely training and testing. This research aims to obtain the best CNN model for breast cancer classification based on mammogram images. The following is the flowchart of this study.

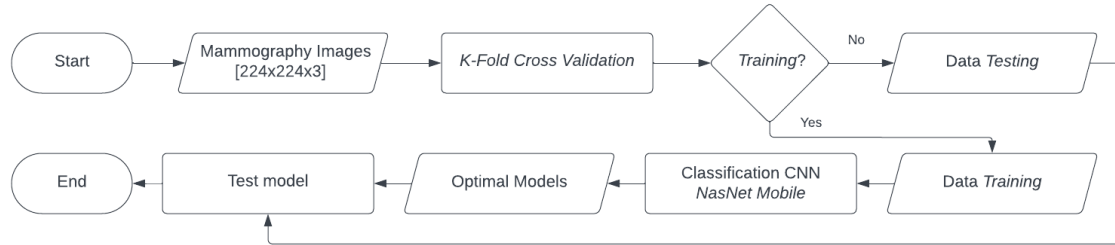


Figure 1 Methodology flowchart process.

2.1 Dataset

Secondary data of mammogram images for breast cancer were retrieved from the website <https://www.kaggle.com/datasets/kmader/mias-mammography> under the title 'MIAS Mammography' and utilized in this study [18]. The dataset consists of 322 images categorized into three classes: 207 images of standard cases, 64 images of benign tumors, and 51 images of malignant tumors, as illustrated in **Figure 2**. One of the advantages of this dataset is the apparent visual distinction between classes (benign, malignant, and regular), which contributes to the classification results despite data imbalance. In addition, although the data is classified as imbalance data, with the comparison of the smallest class (51 images) and the largest class (207 images) is still greater than 1:10. It can be said that the difference is not extreme, so it does not require special handling of imbalance data.

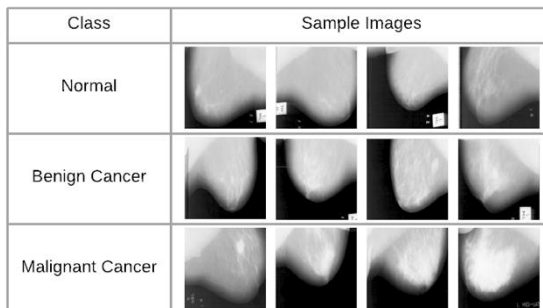


Figure 2 Sample of Mammography Images Dataset

2. 2 Pre-processing

The first pre-processing stage involves converting raw data from grayscale to RGB images. The second stage in this study is resizing the images to 224x224x3 pixels using the Bicubic interpolation method. It is conducted to meet the input requirements of NASNet Mobile. Bicubic interpolation is a more sophisticated method that produces smoother results along the edges than bilinear interpolation. Bicubic interpolation uses a 4x4 pixel neighborhood to gather information, resulting in sharper images compared to bilinear and nearest neighbor methods [16].

2. 3. K-Fold Cross Validation

The classification system requires training and testing data, where training data plays a role in discovering patterns within the data, and testing data play a role in obtaining classification results using the identified patterns. *K*-fold Cross Validation is one of the methods used to split data into training and testing sets. Additionally, this method evaluates the classification system performance by randomly dividing the data into *k* subsets, where *k* is more

significant than one and does not exceed the total number of data points. The data grouping is performed by iterating k times, where each iteration produces one group of testing data and the remaining data as training data. The illustration of k -fold cross-validation is shown in **Figure 3**. [17]

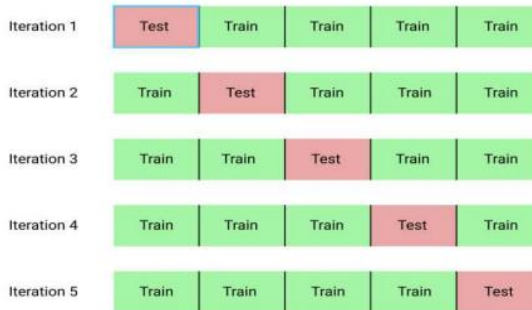


Figure 3 The illustration of K-Fold Cross Validation

2. 4. Convolutional Neural Network (CNN)

Convolutional Neural Network (CNN), also known as ConvNet, utilizes techniques such as weighted sharing, downsampling, and local connection to reduce the required parameters and decrease the complexity level of neural networks. The CNN architecture consists of two main stages: the feature learning stage and the classification stage, as depicted in **Figure 4**. [19]

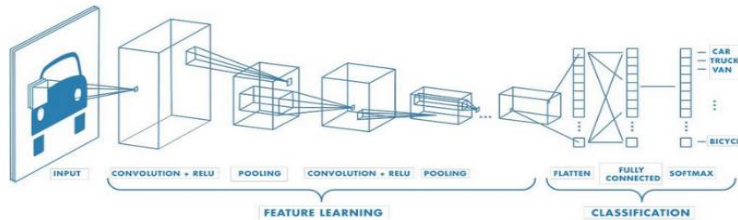


Figure 4 Architecture CNN

CNN consists of three common elements in feature learning: the convolution layer, ReLU, and the pooling layer. In the convolutional layer, a kernel extracts features from the input image. ReLU makes training effective and efficient by setting negative output values to 0 while preserving positive values. The pooling layer simplifies the size of the feature map. Classification is the output of the feature map in a multi-dimensional form. Thus, flattening is necessary by transforming the matrix from the feature map into a vector shape to serve as input for the fully connected (FC) layer. Subsequently, the FC layer applies the softmax activation function to generate probability values for each class [20].

2. 5. NASNet Mobile

NASNet is a CNN architecture built through neural architecture search, consisting of fundamental building blocks (cells) optimized using reinforcement learning [21]. The NASNet Mobile architecture in **Figure 5** is one variant of NASNet, and its development is focused explicitly on embedded systems and mobile devices.

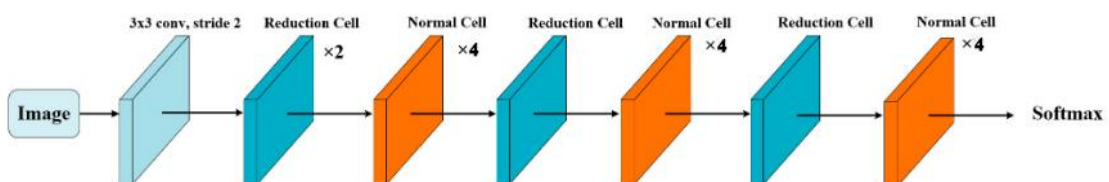


Figure 5 Architecture NASNet Mobile

The embedded system in NASNet Mobile represents the capability of this network architecture to operate effectively on mobile devices while maintaining high prediction quality and resource efficiency. The input image dimensions for this network are (224, 224, 3). The NASNet Mobile model has 913 layers with 5.3 million parameters, and there are approximately 1056 nodes used in the fully connected layers. The NASNet Mobile layer has two types of convolutional cells used when using feature maps as input: normal cells and reduction cells. Normal cells define the size of the feature map, while reduction cells reduce the height and width of the feature map [22]. The architectures of normal and reduction cells are illustrated in **Figure 6** and **Figure 7**.

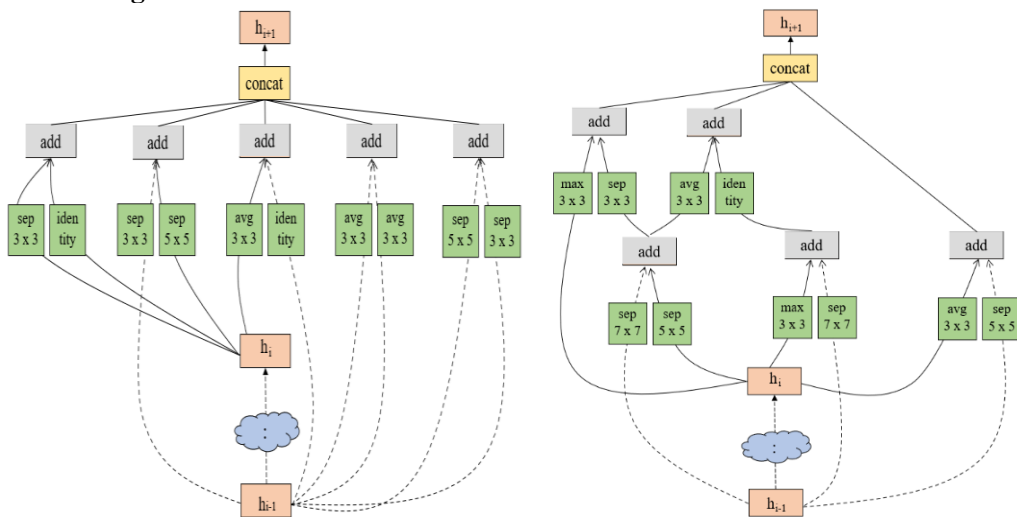


Figure 7 Architecture Normal Cells (left) and Architecture Reduction Cells (right).

2. 6. Performance Evaluation

The confusion matrix plays a role in measuring a model's performance evaluation of a model by comparing actual values and predicted values [23]. The desired outcome of classification is a low error rate and the accuracy of the expected classification results. Therefore, to assess the success rate of the classification system, an evaluation of the system is necessary. Three indicators are used for system evaluation with the confusion matrix: accuracy, sensitivity, and specificity. The values of these parameters can be determined using Equations (1) to (3).

$$\text{Accuracy} = (\text{TP} + \text{TN}) / (\text{TP} + \text{TN} + \text{FP} + \text{FN}) \times 100\% \quad (1)$$

$$\text{Sensitivity} = \text{TP} / (\text{TP} + \text{FP}) \times 100\% \quad (2)$$

$$\text{Specificity} = \text{TN} / (\text{TN} + \text{FP}) \times 100\% \quad (3)$$

Where TP is the True Positive value, TN is the True Negative value, FP is the False Positive value, and FN is the False Negative value.

3. RESULTS AND DISCUSSION

The initial stage of this research is the pre-processing stage. Pre-processing enhances the data that will be utilized before feature extraction. The image data used has dimensions of 1024x1024x3 pixels. The NASNet model requires image data input with dimensions of 224x224x3 pixels, necessitating the resizing of images for the learning stage. In the pre-processing stage of this research, the resize process will adjust the size of the images from 1024x1024x3 pixels to 224x224x3 pixels. The illustration of the image resize process is shown in **Figure 8**.

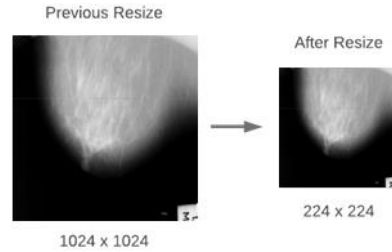


Figure 8 Illustration of the image resizing process

After resizing all images to 224 x 224 pixels, the next step involves splitting the data into training and testing sets using K-Fold cross-validation with a value of $k = 5$, as illustrated in **Figure 9**.

```

r;clc;
= imagedatastore('C:\Users\HP\Documents\SKRIPSI\

l = imds.Labels;
5;
crossvalind('Kfold',Label,k);
i = 1:k
d = b==i;
Test{i} = imds.Files(find(d));
LabelTest{i} = imds.Labels(find(d));
Train{i} = imds.Files(find(~d));
LabelTrain{i} = imds.Labels(find(~d));

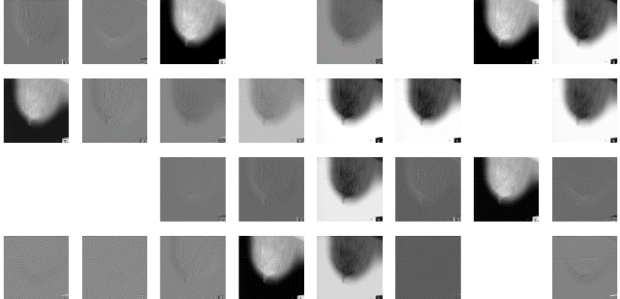
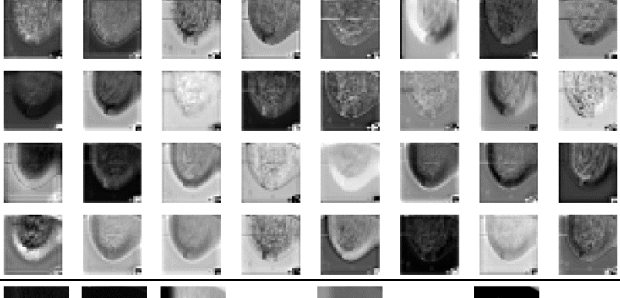
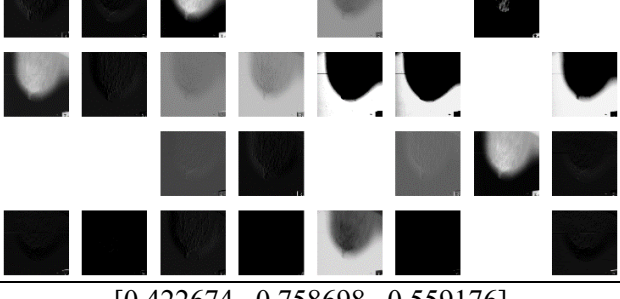
```

Figure 9 K-Fold Cross Validation.

K-Fold Cross Validation with a value of $k = 5$, the training data ranges from 289 to 290, while the testing data ranges from 32 to 33. In the case of $k = 10$, the training data ranges from 257 to 258, and the testing data ranges from 64 to 65. The larger the value of k , the more data for the training process and the less data for the testing process. After splitting the data into training and testing sets, the classification process will be carried out using the NASNet Mobile method. **Table 1** presents an example of the output for each layer in NASNet Mobile.

Table 1 Example outputs for each layer NASNet Mobile.

Name of layer	Output								Size
Input Layer									(224 x 224 x 3)
Convolution Layer									(111 x 111 x 32)

Name of layer	Output								Size
Batch Normalization Layer									(111 x 111 x 32)
NASNet Layer									(7 x 7 x 176)
ReLU Layer									(7 x 7 x 1056)
Global Average Pooling Layer	[0.422674 0.758698 0.559176]								(1 x 1 x 1056)
Fully Connected Layer	[0.038566 0.592597 0.870472]								(1 x 1 x 1000)
Softmax Layer	[0.000401 0.001872 0.001091]								

The formation of the classification system in the study involves two processes: training and testing. The hyperparameters used for training and testing in this study are shown in **Figure 11**.

```
miniBatchSize = 16;
valFrequency = floor(numel(imdsTrain.Files)/miniBatchSize);

options = trainingOptions('rmsprop', ...
    'MiniBatchSize',miniBatchSize, ...
    'MaxEpochs',5, ...
    'InitialLearnRate',3e-4, ...
    'Shuffle','every-epoch', ...
    'ValidationData',augimdsValidation, ...
    'ValidationFrequency',valFrequency, ...
    'Verbose',false, ...
    'Plots','training-progress');
tic;
```

Figure 11 NASNet Mobile training data process.

This code configures the training settings for the deep learning model. Using RMSprop as the optimization algorithm, with a mini-batch size of 16 and a maximum of 5 epochs, the model will be trained with shuffled data for every epoch. The augmented validation data will be

evaluated at specific intervals during training. These options are summarized in the 'options' object. The 'tic' function is used to measure the training time. The goal of this configuration is to achieve efficient and optimal model training. The training and testing results of NASNet Mobile are presented in **Figure 12**.



Figure 12 Train versus test accuracy of NASNet Mobile model

In **Figure 12**, the x-axis represents iterations or epochs, while the y-axis represents evaluation metrics plotted, such as loss or accuracy. The performance results include accuracy and loss values during the training process of image data. The accuracy reaches a percentage greater than 90%, while the total loss value stays below 0.5. Overall, the graph above shows that the model is experiencing an increasing performance trend in terms of accuracy and a decreasing loss trend as the iterations or epochs increase. The rising accuracy graph shows the model's ability to recognize essential patterns in the data and make more accurate predictions. In contrast, the decreasing loss graph shows that the model is getting closer to better representing the data. This indicates that the model is learning well and producing better predictions over time.

The model is evaluated using a Confusion Matrix based on accuracy, sensitivity, and specificity percentage values. **Table 2** shows the results of the parameter test using NASNet Mobile.

Table 2 Result based on several parameters using NASNet Mobile

Batch Size	Accuracy (%)	Sensitivity (%)	Specificity (%)	Training Time
4	98.09	95.35	98.73	60 m 25 s
8	99.08	96.78	95.28	42 m 19 s
16	99.67	99.04	98.11	31 m 33 s
32	98.21	91.84	98.09	28 m 52 s

In the test table, the most optimal model was found with the fastest computational time using a batch size of 16, achieving accuracy, sensitivity, and specificity percentages of 99.67%, 98.78%, and 99.35%, respectively, with a training time of 31 minutes and 33 seconds. The training time column indicates that the required computational time becomes faster as the batch size increases. A batch size of 16 appears to effectively balance learning stability and data exposure, enabling the model to capture subtle visual differences between classes. Smaller batch sizes may increase sensitivity to noise, while larger ones can lead to underfitting. This batch size also aligns well with the hardware capacity, supporting efficient training and smooth model convergence. This differs from the findings of Radiuk's research [24], which stated that smaller batch sizes result in faster computational times. The confusion matrix results are shown in **Figure 13**.

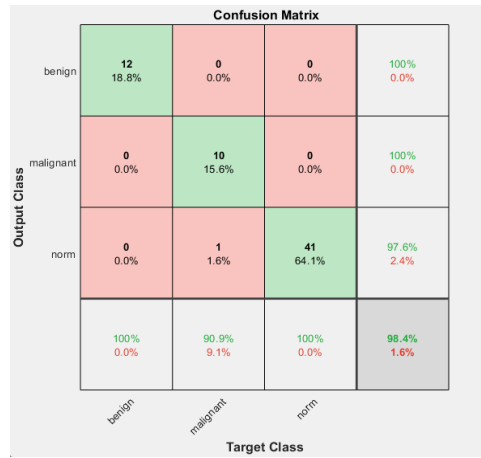


Figure 13 Confusion Matrix of NASNet Mobile result.

Figure 13 shows the confusion matrix of the model's performance in classifying three categories of mammogram images: normal, benign, and malignant. All 12 benign and 10 malignant cases were correctly classified, achieving 100% accuracy for both categories. Out of 42 normal images, 41 were correctly recognized, with only one misclassified as malignant, resulting in an overall accuracy of 98.4%. These results demonstrate the model's strong ability to distinguish between the categories with high sensitivity and specificity across all classes. Despite the class imbalance, the model performed well, showcasing its effectiveness in real-world diagnostic scenarios. Transfer learning with NASNet Mobile, trained on large datasets like ImageNet, enhanced the model's ability to extract relevant features, even for minority classes.

The high sensitivity and specificity values indicate the model's strong diagnostic capability. Sensitivity measures how well the model identifies individuals with the condition, while specificity helps reduce false positives, providing confidence in negative results. In medical applications, these qualities are crucial for accurate, early detection of diseases. Thus, the NASNet Mobile model for mammogram image classification can be considered highly accurate in detecting breast cancer.

The optimal architecture model from several parameter experiments is then used to apply the breast cancer classification system. The classification results detected by this system include three classes: detected as normal or disease-free, benign cancer, and malignant cancer. Examples of classification results for each class are shown in **Figure 14**, **Figure 15**, and **Figure 16**.

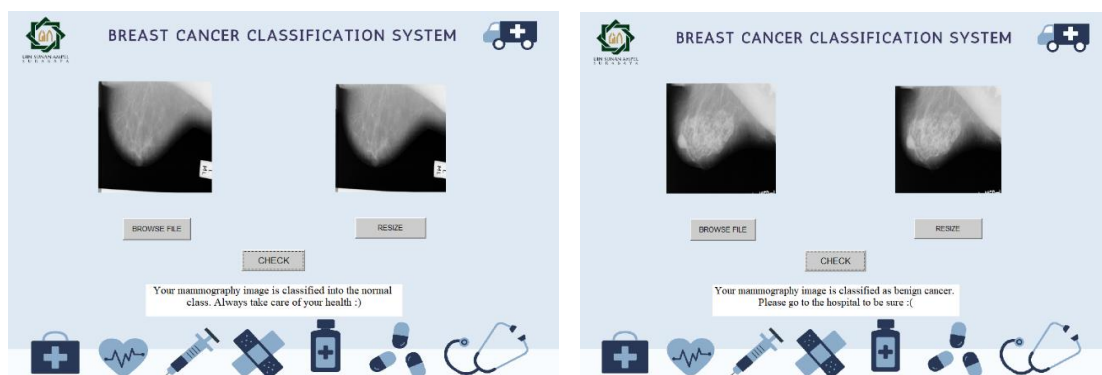


Figure 15 Example Classification Results for the Benign Cancer Class (left). **Figure 14** Example Classification Results for the Normal Class (right)

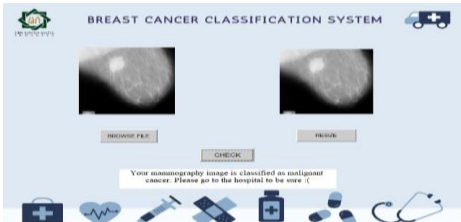


Figure 16 Example Classification Results for the Malignant Cancer Class

By using this application, mammogram image data processing can be carried out efficiently and accurately, assisting medical professionals in making informed decisions in a shorter time. It will facilitate and enhance efficiency in diagnosing and managing breast cancer. **Table 3** compares the proposed dataset with other datasets that use the NASNet Mobile method.

Table 3 Summary of the different databases for NASNet Mobile

Authors	Dataset	Accuracy
Ahsan [25]	CT-scan	82,94%
	X-ray	93,94%
Proposed database	Mammography	98,44%

Ahsan [25] applied the NASNet Mobile model to CT-scan data, achieving an accuracy of 82.94% and 93.94% on X-ray data. In contrast, in this study, the performance of NASNet Mobile using mammography databases achieved the highest accuracy of 98.44%. It indicates that the model's performance can be influenced by the type of data used. Although the model used is the same, differences in data characteristics, such as image resolution, object diversity, or clarity level, can also affect the model's performance in recognizing patterns and making accurate predictions. Therefore, the selection of the most suitable type of data for the analysis goal becomes crucial.

The performance of the cancer classification system on mammograms is closely related to the method used. To better understand the performance of the proposed method, a comparison with other approaches is needed. However, making this comparison is not easy for several reasons. Both approaches must be evaluated using similar databases of the same size to allow for an objective comparison of classification methods. **Table 4** compares the proposed method with other approaches using the MIAS database.

Table 4 Summary of different methods for the MIAS database

Authors	Year	Method	Accuracy
Syam J. et al. [26]	2019	GLCM & BPNN	94,06%
Jose Daniel et al. [27]	2020	Inception-v3	86,05%
Salvador et al. [28]	2021	Googlenet	91,92%
Sarmad et al. [6]	2022	TTCNN	96,57%
Proposed methodology	2023	NASNet Mobile	98,44%

Syam Julio et al. [26] conducted classification using a combination of GLCM and BPNN methods on the MIAS database, obtaining an accuracy of 94.06%. The conventional GLCM-BPNN approach is unable to extract features automatically. Jose Daniel et al. [27] used Inception-v3 on the MIAS database, resulting in an accuracy of 86.05%. Salvador et al. [28] used GoogLeNet on the MIAS database, achieving an accuracy of 91.92%. Sarmad et al. [6] used TTCNN on the MIAS database, yielding an accuracy of 96.57%. The performance of the proposed method produces a superior NASNet Mobile model with an accuracy of 98.44%.

Breast cancer classification research based on mammography images using the CNN method with the NASNet Mobile model has made a significant contribution to improving the accuracy of automatic early cancer detection. NASNet Mobile, as an efficient and lightweight CNN architecture, can extract complex visual features from mammography images with high precision, even on devices with limited computing. This approach supports the development of a faster, more accurate, and more accessible diagnostic support system, thus potentially accelerating medical treatment and reducing mortality due to late breast cancer diagnosis.

4. CONCLUSIONS

In this study, we propose using the NASNet Mobile deep learning model for breast cancer classification based on mammogram images, leveraging transfer learning to adapt a pre-trained architecture for more accurate classification. The system showed significant improvements, achieving accuracy, sensitivity, and specificity values of 99.67%, 98.78%, and 99.35%, respectively. These results highlight the model's effectiveness, especially in dense breast tissue, and its strong performance despite the class imbalance in the publicly available dataset. The automatic classification system offers valuable support for radiologists, improving diagnostic accuracy and efficiency.

In recent years, there has been an evolution and shift from conventional methods to deep learning models with automatic and more complex feature learning. From year to year, research aims to optimize models to recognize more complicated features in an image. Simple conventional methods are suitable for small datasets but are less effective in identifying segments in images. On the other hand, deep learning is ideal for larger datasets but also requires more significant resources. For future research, exploring hyperparameter tuning, expanding the dataset with diverse images, and adapting the model for multi-class detection or integrating segmentation methods could further enhance performance and diagnostic accuracy. In addition, integrating model interpretability techniques, such as Grad-CAM, can be explored to increase transparency in model decision-making to support clinical confidence. Model testing on real systems based on mobile devices or edge computing is also a potential direction for implementing fast and affordable breast cancer diagnosis in various health facilities.

REFERENCES

- [1] World Health Organization, *Cancer*. 2022. Accessed: Sep. 13, 2022. [Online]. Available: <https://www.who.int/news-room/fact-sheets/detail/cancer>
- [2] Kementrian Kesehatan RI, *Kanker Payudara Paling Banyak di Indonesia, Kemenkes Targetkan Pemerataan Layanan Kesehatan*. Jakarta, Indonesia: Kementrian Kesehatan RI, 2022. [Online]. Available: <https://www.kemkes.go.id/article/view/22020400002/kanker-payudara-paling-banyak-di-indonesia-kemenkes-targetkan-pemerataan-layanan-kesehatan.html>
- [3] K. S. A. Fazilov Sh. Kh., O. R. Yusupov, *MAMMOGRAPHY IMAGE SEGMENTATION IN BREAST CANCER IDENTIFICATION USING THE OTSU METHOD*, vol. 3, no. 8. 2022.
- [4] S. M. Shah, R. A. Khan, S. Arif, and U. Sajid, *Artificial intelligence for breast cancer analysis: Trends & directions*, vol. 142. 2022. doi: 10.1016/j.combiomed.2022.105221.
- [5] S. Azam *et al.*, *Mammographic microcalcifications and risk of breast cancer*, vol. 125, no. 5. 2021. doi: 10.1038/s41416-021-01459-x.
- [6] S. Maqsood, R. Damaševičius, and R. Maskeliūnas, *TTCNN: A Breast Cancer Detection and Classification towards Computer-Aided Diagnosis Using Digital Mammography in Early Stages*, vol. 12, no. 7. 2022. doi: 10.3390/app12073273.
- [7] M. S. Ejaz and M. R. Islam, *Masked face recognition using convolutional neural network*, vol. 0. IEEE, 2019. doi: 10.1109/STI47673.2019.9068044.
- [8] M. Z. Amin and N. Nadeem, *Convolutional Neural Network: Text Classification Model for Open Domain Question Answering System*. 2018. [Online]. Available:

<http://arxiv.org/abs/1809.02479>

[9] R. N. S. Husna, A. R. Syafeeza, N. A. Hamid, Y. C. Wong, and R. A. Raihan, *Functional magnetic resonance imaging for autism spectrum disorder detection using deep learning*, vol. 83, no. 3. 2021. doi: 10.11113/JURNALTEKNOLOGI.V83.16389.

[10] J. Huixian, *The Analysis of Plants Image Recognition Based on Deep Learning and Artificial Neural Network*, vol. 8. 2020. doi: 10.1109/ACCESS.2020.2986946.

[11] Q. Zhang, J. Lin, H. Song, and G. Sheng, *Fault Identification Based on PD Ultrasonic Signal Using RNN, DNN and CNN*. 2018. doi: 10.1109/CMD.2018.8535878.

[12] L. Wen, X. Li, X. Li, and L. Gao, *A New Transfer Learning Based on VGG-19 Network for Fault Diagnosis*. 2019. doi: 10.1109/CSCWD.2019.8791884.

[13] A. Chavda, J. Dsouza, S. Badgjar, and A. Damani, *Multi-Stage CNN Architecture for Face Mask Detection*. 2021. doi: 10.1109/I2CT51068.2021.9418207.

[14] T. Sadad *et al.*, *Brain tumor detection and multi-classification using advanced deep learning techniques*, vol. 84, no. 6. 2021. doi: 10.1002/jemt.23688.

[15] K. Radhika, K. Devika, T. Aswathi, P. Sreevidya, V. Sowmya, and K. P. Soman, *Performance analysis of NASNet on unconstrained ear recognition*, vol. SCI 871. Springer International Publishing, 2020. doi: 10.1007/978-3-030-33820-6_3.

[16] S. Bharati, P. Podder, M. R. H. Mondal, and N. Gandhi, *Optimized NASNet for Diagnosis of COVID-19 from Lung CT Images*. Cham: Springer International Publishing, 2021.

[17] S. Vallabhajosyula, V. Sistla, and V. K. K. Kolli, *Transfer learning-based deep ensemble neural network for plant leaf disease detection*, vol. 129, no. 3. Springer Berlin Heidelberg, 2022. doi: 10.1007/s41348-021-00465-8.

[18] J. Suckling *et al.*, *The Mammographic Image Analysis Society Digital Mammogram Database*, vol. 1069, no. JANUARY 1994. 1994. [Online]. Available: http://www.researchgate.net/publication/247927550_The_Mammographic_Image_Analysis_Society_Digital_Mammogram_Database”Exerpta Medica

[19] M. Benco, R. Hudec, P. Kamencay, M. Zachariasova, and S. Matuskal, *An advanced approach to extraction of colour texture features based on GLCM*, vol. 11, no. 1. 2014. doi: 10.5772/58692.

[20] Y. Zhang, J. Gao, and H. Zhou, *Breeds Classification with Deep Convolutional Neural Network*, no. 24. 2020. doi: 10.1145/3383972.3383975.

[21] A. O. Adedoja, P. A. Owolawi, T. Mapayi, and C. Tu, *Intelligent Mobile Plant Disease Diagnostic System Using NASNet-Mobile Deep Learning*, vol. 49, no. 1. 2022.

[22] S. K. Addagarla, *Real Time Multi-Scale Facial Mask Detection and Classification Using Deep Transfer Learning Techniques*, vol. 9, no. 4. 2020. doi: 10.30534/ijatcse/2020/33942020.

[23] D. Valero-Carreras, J. Alcaraz, and M. Landete, *Comparing two SVM models through different metrics based on the confusion matrix*, vol. 152, no. April 2022. Elsevier Ltd, 2023. doi: 10.1016/j.cor.2022.106131.

[24] P. M. Radiuk, “Impact of Training Set Batch Size on the Performance of Convolutional Neural Networks for Diverse Datasets,” *Inf. Technol. Manag. Sci.*, vol. 20, no. 1, pp. 20–24, 2018, doi: 10.1515/itms-2017-0003.

[25] M. M. Ahsan, K. D. Gupta, M. M. Islam, S. Sen, M. L. Rahman, and M. Shakhawat Hossain, *COVID-19 Symptoms Detection Based on NasNetMobile with Explainable AI Using Various Imaging Modalities*, vol. 2, no. 4. 2020. doi: 10.3390/make2040027.

[26] S. J. A. Sarosa, F. Utaminingrum, and F. A. Bachtiar, “Breast cancer classification using GLCM and BPNN,” *Int. J. Adv. Soft Comput. its Appl.*, vol. 11, no. 3, pp. 157–172, 2019.

[27] J. Daniel López-Cabrera, L. Alberto López Rodriguez, and M. Pérez-Díaz, “Classification of breast cancer from digital mammography using deep learning,” *Intel. Artif.*, vol. 23, no. 65, pp. 56–66, 2020, doi: 10.4114/intartif.vol23iss65pp56-66.

[28] S. Castro-Tapia *et al.*, “Classification of breast cancer in mammograms with deep learning adding a fifth class,” *Appl. Sci.*, vol. 11, no. 23, 2021, doi: 10.3390/app112311398.